

200 Gbit/s Optical PAM4 Modulation Based on Silicon Microring Modulator

Yuguang Zhang^{(1),(2)}, Hongguang Zhang⁽¹⁾, Miaofeng Li^{(1),(2)}, Peng Feng^{(1),(2)}, Lei Wang^{(1),(2)},
Xi Xiao^{(1),(2)*}, and Shaohua Yu^{(1),(2)}

⁽¹⁾ National Information Optoelectronics Innovation Center, China Information and Communication Technologies Group Corporation (CICT), Wuhan 430074, Hubei, China

⁽²⁾ State Key Laboratory of Optical Communication Technologies and Networks, China Information and Communication Technologies Group Corporation (CICT), Wuhan 430074, Hubei, China

Author e-mail address: xxiao@wri.com.cn

Abstract We present an ultra-high speed silicon microring modulator with the $V_{\pi} \cdot L$ of 0.8 V·cm and the 3-dB electro-optical bandwidth larger than 67 GHz. Using this high-performance and compact modulator, the modulations of 120 Gbit/s NRZ and 200 Gbit/s PAM4 are experimentally demonstrated with the bit error ratios of $1.5e-3$ and $1.08e-3$, respectively.

Introduction

Over the recent years, silicon microring modulators^{[1]-[3]} have been intensively investigated owing to their unique advantages of compact footprint, low optical loss and low power consumption. Silicon microring modulator with the modulation data rate of 100 Gbit/s^[4] has been experimentally demonstrated using four-level pulse amplitude modulation (PAM4). However, there is an intrinsic trade-off between the modulation efficiency and the electro-optical (EO) bandwidth for silicon microring modulator. In order to extend the EO bandwidth without reducing the modulation efficiency, the optical peaking^[5] caused by the intrinsic time dynamics in the silicon microring modulator is researched. Through this approach, high bandwidth silicon microring modulator^[6, 7] with the 3-dB EO bandwidth of 50 GHz is achieved, supporting the modulation data rate of 128 Gbit/s.

In this paper, we present the ultra-high speed silicon microring modulator with the 3-dB EO bandwidth larger than 67 GHz, exceeding the frequency range limit of the lightwave component analyzer (LCA). The high 3-dB EO bandwidth is obtained by combining the optical peaking and optimizing the resistance and the capacitance of the silicon microring modulator. The product of the π -phase-shift voltage and length ($V_{\pi} \cdot L$) and the thermo-optical (TO) tuning efficiency are measured to be 0.8 V·cm and 0.1 nm/mW, respectively. Based on the silicon microring modulator, modulations of 120 Gbit/s NRZ and 200 Gbit/s PAM4 are experimentally achieved with the bit error ratios (BERs) of 1.05×10^{-3} and 1.08×10^{-3} , respectively, below the hard-decision forward error correction (HD-FEC) threshold. To the best of our knowledge, 200 Gbit/s PAM4 modulation is the highest data rate ever reported for silicon microring modulator.

Design and fabrication

The proposed ultra-high speed silicon microring modulator is designed based on the Silicon-On-Insulator (SOI) platform with the thickness of the silicon device layer of 220 nm. The silicon microring modulator is fabricated with standard CMOS process. Figure 1 shows the microscope picture of the fabricated silicon microring modulator. The silicon waveguide is partially etched with the etching depth of 150 nm, forming the waveguide with the width of 420 nm and the slab thickness of 70 nm. The radius of the silicon microring modulator is chosen to be 8 μm . To increase the coupling efficiency, a racetrack with the length of 5 μm is added at the coupling region with the gap of 280 nm. The grating couplers for transverse electric (TE) mode possessing the coupling efficiency of 40% (-4 dB) are used to couple light input and output the device from the optical fibers.

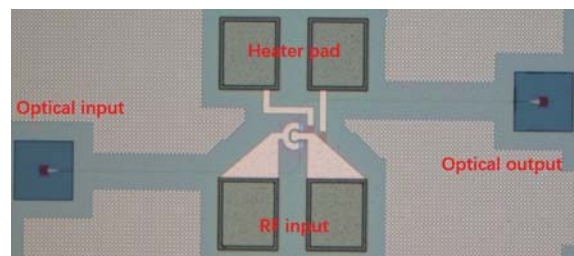


Fig. 1: The microscope picture of the fabricated silicon microring modulator.

Due to the fabrication errors or temperature variations, the resonant wavelength of silicon microring modulator will deviate from the designed value. In order to post-adjust the resonant wavelength, an integrated titanium nitride (TiN) heater is implemented above the silicon microring modulator. A vertical PN junction is placed in the silicon microring modulator, working with depletion mode. For better trade-off between the EO modulation efficiency and the EO bandwidth of the silicon

microring modulator, we optimized the doping density and the position of the PN junction in the waveguide.

Static characterization

To characterize the EO modulation efficiency of the silicon microring modulator, we measured the transmission spectrum at different reversed bias voltages, as shown in Fig. 2(a). From this figure, we can find that as the rise of the reversed bias voltage, the resonant wavelength of the silicon microring modulator red shifts. This is because increasing the reversed bias voltage, the refractive index of the silicon waveguide increases for depletion-mode modulator. Since the silicon microring modulator is lightly under-coupled, rising the reversed bias voltage, the optical loss decreases and the extinction ratio (ER) enlarges. The highest ER of the silicon microring modulator is reached when the reversed bias voltage is 2 V. Then, the silicon microring modulator is over-coupled, therefore, further increasing the reversed bias voltage, the ER will decrease. The measured free spectrum range (FSR) of the silicon microring modulator is 7 nm near the wavelength of 1310 nm, agreeing well with the simulation. The Q factor of the silicon microring modulator is measured to be 5600.

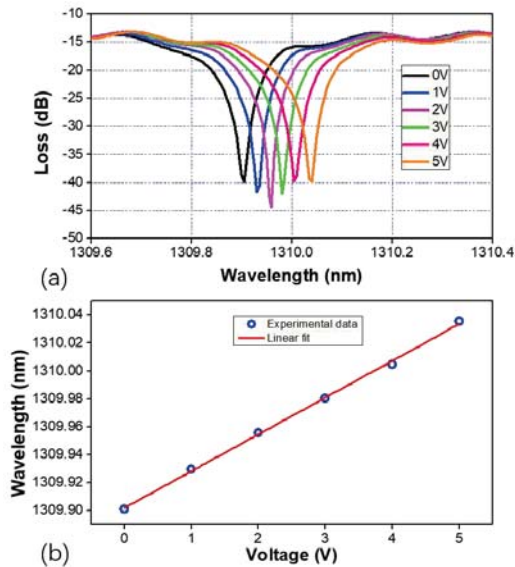


Fig. 2: (a) The measured transmission spectrums of the silicon microring modulator at different reversed bias voltages. (b) The relationship between the resonant wavelengths and the reversed bias voltages. The EO modulation efficiency is calculated to be 26.34 pm/V, indicating the $V_{\pi} \cdot L$ of 0.8 V·cm.

Figure 2(b) shows the resonant wavelengths of the silicon microring modulator at different reversed bias voltages. By linear fitting the resonant wavelengths with the reversed bias voltages, the EO modulation efficiency is calculated to be 26.34 pm/V, which indicates that the $V_{\pi} \cdot L$ of the silicon microring modulator

is about 0.8 V·cm.

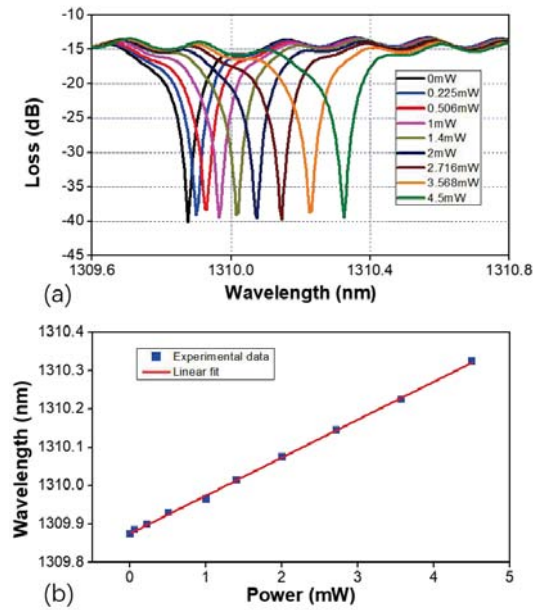


Fig. 3: (a) The transmission spectrums of the silicon microring modulator with different powers applied to the TiN heater. (b) The linear fitting of the resonant wavelengths with the applied powers. The TO efficiency of the TiN heater is calculated to be 0.1 nm/mW, which means that the half-wave power P_{π} will be 35 mW.

The performance of the TiN heater is also investigated by measuring the transmission spectrums of the silicon microring modulator with different powers implemented to the TiN heater, as shown in Fig. 3(a). Due to the TO coefficient of silicon, the resonant wavelength of the silicon microring modulator red shifts as the increase of the applied power. The relationship between the resonant wavelengths and the applied powers is shown in Fig. 3(b). The TO efficiency of the TiN heater is calculated to be 0.1 nm/mW, which means that the half-wave power P_{π} will be 35 mW. The low TO efficiency of the TiN heater is due to both the short heater length and the high thermal conductivity of silicon. Therefore, we can further improve the TO efficiency of the TiN heater by insulating the silicon microring modulator through substrate removing.

The small-signal EO response of the proposed silicon microring modulator is characterized by high speed LCA with the frequency range of 67 GHz. In order to accurately measure the EO response, we de-embedded the responses of the cables and the probe through standard LCA calibrations. Figure 4 shows the measured EO response (S_{21}) of the silicon microring modulator with the reversed bias voltage of 2 V. Since the intrinsic time dynamics of the silicon microring modulator, there will be an optical peaking around 50 GHz for the EO response, beyond the photon lifetime

limited bandwidth of 41 GHz. The measured 3-dB EO bandwidth of the silicon microring modulator is larger than 67 GHz, limited by the frequency range of the LCA. And the 3-dB EO bandwidth of the silicon microring modulator is predicted to be 79 GHz.

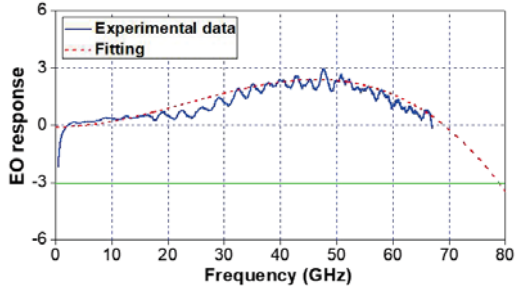


Fig. 4: The measured EO response of the high-speed silicon microring modulator. The 3-dB EO bandwidth is larger than 67 GHz, limited by the frequency range of the LCA.

High speed characterization

Then, we carried out the NRZ and PAM4 signal modulations based on the silicon microring modulator. The output light with the power of 15 dBm from the tunable laser is coupled to the silicon microring modulator through the grating coupler. The NRZ and PAM4 signal with the word length of $2^{15} - 1$ are generated by the arbitrary wave generator (AWG) with the sampling rate of 120 GS/s. After amplified with a linear RF driver, the NRZ and PAM4 signals are connected to the silicon microring modulator by a high bandwidth G-S probe. Meanwhile, a bias tee is used to provide the DC bias with the reversed bias voltage of 4 V. The output optical signal from the silicon microring modulator with the power of 2.5 dBm is converted to electrical signal by a commercial photodetector with the 3-dB bandwidth of 50 GHz. Since the low optical power, we used another linear driver to amplify the converted electrical signal. Finally, a real-time digital storage oscilloscope (DSO) with the sampling rate of 256 GS/s is used to capture the amplified electrical signal, and the BERs of the NRZ and PAM4 signal are calculated through the off-line digital signal processing (DSP) as described in our previous work^[8].

The BERs of the NRZ signal and the PAM4 signal with different data rates are presented in Fig. 5(a) and 5(b), respectively. The inset pictures in Fig. 5(a) and 5(b) show the optical eye diagrams with the data rates of 110 Gbit/s NRZ and 200 Gbit/s PAM4, respectively. The BERs of 120 Gbit/s NRZ and 200 Gbit/s PAM4 are calculated to be $1.05e-3$ and $1.08e-3$, respectively, below the HD-FEC threshold. The BER of 220 Gbit/s PAM4 is $2.27e-2$, lightly higher than the soft-decision FEC (SD-FEC) threshold. We believe that the BERs of the NRZ

signal and the PAM4 signal can be further reduced by replacing the grating couplers with the spot-size couplers featuring higher coupling efficiency. In this way, the second linear driver can be removed to reduce the noise.

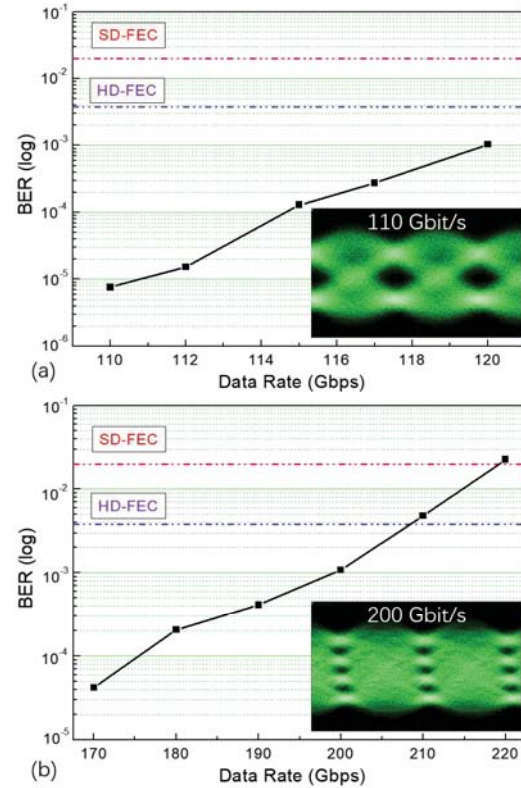


Fig. 5: (a) The measured BERs with different data rates for NRZ modulation. Inset: The optical eye diagram with the data rate of 110 Gbit/s NRZ. (b) The measured BERs with different data rates for PAM4 modulation. Inset: The optical eye diagram with the data rate of 200 Gbit/s PAM4.

Conclusions

By optimizing the PN junction and utilizing the optical peaking effect, we experimentally demonstrated the ultra-high speed silicon microring modulator. The 3-dB EO bandwidth is measured to be larger than 67 GHz, limited by the frequency range of the LCA. The $V_{\pi} \cdot L$ and the TO tuning efficiency of the silicon microring modulator are calculated to be $0.8 \text{ V} \cdot \text{cm}$ and 0.1 nm/mW , respectively. Based on the silicon microring modulator, modulations of 120 Gbit/s NRZ and 200 Gbit/s PAM4 are experimentally achieved with the BERs of $1.05e-3$ and $1.08e-3$, respectively, below the HD-FEC threshold. The measured results indicate that the ultra-high speed silicon microring modulator has great potential to be used in the next generation optical interconnect.

Acknowledgements

This work is supported by the National Key Research and Development project of China (2019YFB2205203, 2019YFB2205201); Hubei technological innovation project (2019AAA054).

References

- [1] Q. Xu, B. Schmidt, S. Pradhan, and M. Lipson, "Micrometre-scale silicon electro-optic modulator", *Nature*, vol. 435, pp. 325, 2005.
- [2] P. Dong, S. Liao, D. Feng, H. Liang, D. Zheng, R. Shafiqi, C.-C. Kung, W. Qian, G. Li, X. Zheng, A. V. Krishnamoorthy, and M. Asghari, "Low Vpp, ultralow-energy, compact, high-speed silicon electro-optic modulator", *Opt. Express*, vol. 17(25), pp. 22484-22490, 2009.
- [3] X. Xiao, H. Xu, X. Li, Y. Hu, K. Xiong, Z. Li, T. Chu, Y. Yu, and J. Yu, "25 Gbit/s silicon microring modulator based on misalignment-tolerant interleaved PN junctions", *Opt. Express*, vol. 20(3), pp. 2507-2515, 2009.
- [4] Y. Ban, J. Verbist, M. Vanhooecke, J. Bauwelinck, P. Verheyen, S. Lardenois, M. Pantouvaki, and J. Van Campenhout, "Low-Voltage 60Gb/s NRZ and 100Gb/s PAM4 O-band Silicon Ring Modulator", *IEEE Optical Interconnects Conference*, 2019.
- [5] J. Muller, F. Merget, S. S. Azadeh, J. Hauck, S. R. Garcia, B. Shen, and J. Witzens, "Optical peaking enhancement in high-speed ring modulators," *Scientific Reports*, vol. 4, pp. 6310, 2014.
- [6] J. Sun, R. Kumar, M. Sakib, J. B. Driscoll, H. Jayatileka, and H. Rong, "A 128 Gb/s PAM4 Silicon Microring Modulator with Integrated Thermo-optic Resonance Tuning", *Journal of Lightwave Technology*, vol. 37(1), pp. 110-115, 2019.
- [7] H. Li, G. Balamurugan, M. Sakib, J. Sun, J. Driscoll, R. Kumar, H. Jayatileka, H. Rong, J. Jaussi, and B. Casper, "A 112 Gb/s PAM4 Transmitter with Silicon Photonics Microring Modulator and CMOS Driver", *Optical Fiber Communications Conference and Exhibition*, Th4A.4, 2019.
- [8] Y. Zhang, M. Xu, H. Zhang, M. Li, J. Jian, M. He, L. Chen, L. Wang, X. Cai, X. Xiao, and S. Yu, "220 Gbit/s optical PAM4 modulation based on lithium niobate on insulator modulator", *European Conference on Optical Communication*, PD2.6, 2019.